

Investigation of the Local Geometry and EPR Parameters of V^{3+} and Cr^{4+} Centers in Al_2O_3 Crystals

Wen-Lin Feng^{a,c}, Xiao-Xuan Wu^{b,c,d}, Fang Wang^c, and Wen-Chen Zheng^{c,d}

^a Department of Applied Physics, Chongqing Institute of Technology, Chongqing 400050, P. R. China

^b Department of Physics, Civil Aviation Flying Institute of China, Guanghan 618307, P. R. China

^c Department of Material Science, Sichuan University, Chengdu 610064, P. R. China

^d International Centre for Materials Physics, Chinese Academy of Sciences, Shengyang 110016, P. R. China

Reprint requests to W.-L. F.; Fax: +86 28 85416050; E-mail: wenlinfeng@126.com

Z. Naturforsch. **61a**, 691–694 (2006); received August 8, 2006

The EPR parameters (zero-field splitting D and g factors g_{\parallel} , g_{\perp}) of $3d^2$ V^{3+} and Cr^{4+} centers in Al_2O_3 crystals are calculated by using the diagonalization of the complete energy matrix for $3d^2$ ions in trigonal symmetry. The crystal-field parameters are estimated for the superposition model related to the local geometry (or structure) of the impurity centers. From the calculations, the EPR parameters for both impurity centers are explained and the local structures (characterized by the impurity displacement Δz along the C_3 axis and the displacement Δx of O^{2-} ions in the oxygen triangle between the impurity and the vacant oxygen octahedron along the x -axis, resulting from the electrostatic repulsive force and the electronic cloud overlap) of these impurity centers are estimated. The results are discussed.

Key words: Electron Paramagnetic Resonance; Defect Structure; Crystal-Field Theory; V^{3+} ; Cr^{4+} ; Al_2O_3 .

1. Introduction

Corundum (Al_2O_3) crystals doped with transition metal ions have attracted much attention for a wide variety of applications in laser devices [1–4]. Transition metal ions in Al_2O_3 substitute for the Al^{3+} ions. Since the size and/or charge of the impurity are unlike those of the replaced host ion, impurity-induced local lattice relaxation can occur, and so the local geometry (or structure) of the impurity center in Al_2O_3 may be different from the corresponding structure in

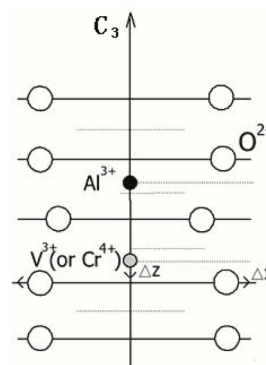


Fig. 1. The defect structure of V^{3+} (or Cr^{4+}) in Al_2O_3 crystal.

the host Al_2O_3 crystal. For technical applications it is necessary to study the local structure of the impurity center because the impurities change the electric, magnetic and optical properties of crystals. Since the EPR parameters of a paramagnetic ion in crystals are sensitive to its immediate environment, information on the local structure of transition metal ions in crystals can be obtained by analyzing their EPR data. The EPR parameters (zero-field splitting D and g factors g_{\parallel} , g_{\perp}) of V^{3+} and Cr^{4+} ions in Al_2O_3 were measured in [5–8]. In the present paper we calculate these EPR parameters by diagonalizing the complete energy matrix for $3d^2$ ions in trigonal symmetry. On the basis of the calculations, the local structures of V^{3+} and Cr^{4+} impurity centers in Al_2O_3 crystals are estimated. The results are discussed.

2. Calculation

The Al_2O_3 structure consists of trigonal oxygen octahedra along the C_3 axis, sharing faces. The centers of the octahedra are occupied by cations in the sequence Al^{3+} , Al^{3+} and a vacant octahedron [9]. The electrostatic repulsive forces between an Al^{3+} pair shift them from the centers of these octahedra, so that the Al^{3+} ions are closer to the neighboring vacancies, and the oxygen triangle closer to the Al^{3+} ion is larger owing to the electronic cloud overlap (see Fig. 1). When the Al^{3+} ion is replaced by an impurity having more charge and/or a larger ionic radius, such as V^{3+} or Cr^{4+} , the electrostatic repulsive force acting on the impurity (and also on the neighboring Al^{3+} ion) becomes larger and so the impurity should be displaced by an amount Δz towards the neighboring vacant octahedron.

Also, the oxygen triangle between the impurity and vacant octahedron is larger (characterized by the O^{2-} displacement Δx along x -axis, see Fig. 1) because of the electron cloud overlap. In this case, the local symmetry of the impurity center is still trigonal. Thus, the Hamiltonian of a $3d^2$ ion in this system (trigonal symmetry) can be expressed as

$$H = H_e(B, C) + H_{so}(\zeta) + H_{cf}(Dq, D\sigma, D\tau) \quad (1)$$

where H_e , H_{so} and H_{cf} are, respectively, the electrostatic interaction (characterized by the Racah parameters B and C), the spin-orbit interaction (characterized by the spin-orbit coupling parameter ζ) and the crystal-field interaction (characterized by the crystal-field parameters Dq , $D\sigma$ and $D\tau$). By using the strong-field basis functions [10], the complete energy matrix for $3d^{2/8}$ ions in trigonal symmetry can be obtained. Diagonalizing the complete energy matrix, one finds that the ground orbital state $t_2^3T_1$ is split into two states, the eigenfunctions of which are $|t_2^3T_10a_0\rangle'$ and $|t_2^3T_1 \pm 1a_0\rangle'$ [11].

The spin Hamiltonian, used to analyze the EPR spectra of $3d^n$ ions in trigonal symmetry, is [12]

$$H_s = g_{\parallel}\mu_B H_z S_z + g_{\perp}\mu_B (H_x S_x + H_y S_y) + D \left[S_z^2 - \frac{1}{3}S(S+1) \right]. \quad (2)$$

Considering the equivalence between the spin Hamiltonian (or EPR) parameters and the complete diagonalization procedure, the calculated formulas of the EPR parameters D , g_{\parallel} and g_{\perp} can be written as [11]

$$\begin{aligned} D &= E(|t_2^3T_1 \pm 1a_0\rangle') - E(|t_2^3T_10a_0\rangle'), \\ g_{\parallel} &= \langle t_2^3T_11a_0 | k l_z + g_s S_z | t_2^3T_11a_0 \rangle', \\ g_{\perp} &= \sqrt{2} \langle t_2^3T_10a_0 | k l_x + g_s S_x | t_2^3T_11a_0 \rangle', \end{aligned} \quad (3)$$

in which k is the orbital reduction factor and g_s (≈ 2.0023) is the free-electron value.

In the above matrix and formulas, the Racah parameters B and C are estimated from the optical spectra of the studied system. Because of the covalency reduction effect for $3d^n$ clusters, the parameters B , C and the spin-orbit coupling parameter ζ for a $3d^n$ ion in crystals are smaller than the corresponding B_0 , C_0 and ζ_0 for $3d^n$ ions in free state [13, 14]. So, we introduce a covalency reduction factor $N = \left(\sqrt[4]{B/B_0} + \sqrt[4]{C/C_0} \right) / 2$ to denote the covalency reduction effect. Thus, we have [15, 16]

$$\zeta \approx N^2 \zeta_0, \quad k \approx N^2. \quad (4)$$

From the superposition model [17], the crystal-field parameters can be given as

$$\begin{aligned} Dq &= \frac{3}{\sqrt{2}} \bar{A}_4(R_0) \sum_{i=1}^2 \left(\frac{R_0}{R_i} \right)^{t_4} \sin^3 \theta_i \cos \theta_i, \\ D\tau &= -\frac{1}{7} \bar{A}_4(R_0) \sum_{i=1}^2 \left(\frac{R_0}{R_i} \right)^{t_4} (35 \cos^4 \theta_i - 30 \cos^2 \theta_i \\ &\quad + 3 + 7\sqrt{2} \sin^3 \theta_i \cos \theta_i), \\ D\sigma &= -\frac{3}{7} \bar{A}_2(R_0) \sum_{i=1}^2 \left(\frac{R_0}{R_i} \right)^{t_2} (3 \cos^2 \theta_i - 1), \end{aligned} \quad (5)$$

where the power-law exponents are $t_2 \approx 3$ and $t_4 \approx 5$ [17–19]. $\bar{A}_2(R_0)$ and $\bar{A}_4(R_0)$ are the intrinsic parameters with the reference distance R_0 . R_i ($i = 1, 2$) is the impurity-ligand distance and θ_i is the angle between R_i and the C_3 axis. For the studied V^{3+} and Cr^{4+} centers in Al_2O_3 crystals, the structural parameters R_i and θ_i can be calculated from the structural data $R_1^h \approx 1.966 \text{ \AA}$, $R_2^h \approx 1.857 \text{ \AA}$, $\theta_1^h \approx 47.7^\circ$ and $\theta_2^h \approx 63.1^\circ$ of the host Al_2O_3 crystal [9] and the above displacements Δz and Δx .

2.1. Calculation for $Al_2O_3:V^{3+}$

From the optical spectra of $Al_2O_3:V^{3+}$ [9, 20, 21], we estimate $B \approx 420 \text{ cm}^{-1}$, $C \approx 2600 \text{ cm}^{-1}$ and $\bar{A}_4(R_0) \approx 1500 \text{ cm}^{-1}$ with $R_0 \approx (R_1^h + R_2^h) / 2 \approx 1.912 \text{ \AA}$. According to the values of $B_0 \approx 861 \text{ cm}^{-1}$, $C_0 \approx 4165 \text{ cm}^{-1}$ and $\zeta_0 \approx 209 \text{ cm}^{-1}$ for a free V^{3+} ion [13], we have $N \approx 0.8578$ and so $\zeta \approx 154 \text{ cm}^{-1}$ and $k \approx 0.736$. The ratio $\bar{A}_2(R_0) / \bar{A}_4(R_0) \approx 9 \sim 12$ is obtained for $3d^n$ ions in many crystals [18, 19, 22]; we take $\bar{A}_2(R_0) / \bar{A}_4(R_0) \approx 12$ here. Thus, in the above matrix and formulas only the displacements Δz and Δx are not known. By fitting the calculated EPR parameters D , g_{\parallel} , g_{\perp} to the experimental values, we obtain for the V^{3+} center in an Al_2O_3 crystal

$$\Delta z \approx 0.2562 \text{ \AA}, \quad \Delta x \approx 0.01 \text{ \AA}. \quad (6)$$

The calculated EPR parameters are compared with the experimental values in Table 1.

2.2. Calculation for $Al_2O_3:Cr^{4+}$

For a Cr^{4+} ion in an Al_2O_3 crystal no optical spectral data have been reported. We can reasonably es-

	D (cm ⁻¹)		g_{\parallel}		g_{\perp}	
	Calc.	Exp.	Calc.	Exp.	Calc.	Exp.
Al ₂ O ₃ :V ³⁺	8.296	8.296(16) [5,6]	1.930	1.910(5) [5,6]	1.655	1.4 ~ 1.7 [5, 6]
		8.25(2) [7]		1.92(3) [7]		1.74(1) [7]
		~ 7 [8]		1.915 [8]		1.63 [8]
Al ₂ O ₃ :Cr ⁴⁺	7.561	7.562(16) [5, 6]	1.909	1.913(5) [5,6]	1.669	1.2 ~ 2.0 [5,6]

Table 1. EPR parameters of V³⁺ and Cr⁴⁺ ions in Al₂O₃ crystals.

estimate the parameters N and $\bar{A}_4(R_0)$ from the corresponding parameters of the isoelectronic V³⁺ ion in Al₂O₃. For the isoelectronic 3d^{*n*} series in a crystal, the covalence increases and hence the covalence reduction factor N decreases with increasing valence of the 3d^{*n*} ion [14]. So the parameter N for Cr⁴⁺ in Al₂O₃ is smaller than that for V³⁺ in Al₂O₃. Thus we take $N \approx 0.8$ for Al₂O₃:Cr⁴⁺. The parameters are $B_0 \approx 1039$ cm⁻¹, $C_0 \approx 4238$ cm⁻¹ and $\zeta_0 \approx 327$ cm⁻¹ for a free Cr⁴⁺ ion [13], thus we have [23] $B \approx N^4 B_0 \approx 426$ cm⁻¹, $C \approx N^4 C_0 \approx 1736$ cm⁻¹, $\zeta \approx N^2 \zeta_0 \approx 209$ cm⁻¹ and $k \approx 0.64$ for an Al₂O₃:Cr⁴⁺ crystal. The crystal-field strength and hence the parameters Dq and $\bar{A}_4(R_0)$ (in the cubic approximation, $Dq \approx 4\bar{A}_4(R_0)/3$ [17–19]) increase with increasing valence state for isoelectronic 3d^{*n*} ions in a crystal [14, 24]. From the linear trends, aiding the interpretation and prediction of optical spectra of 3d^{*n*} ions in crystals [24], we can reasonably estimate $\bar{A}_4(R_0)(Cr^{4+}) \approx 1.3\bar{A}_4(R_0)(V^{3+}) \approx 1950$ cm⁻¹ in Al₂O₃:Cr⁴⁺. Substituting these parameters into the above matrix and formulas, we find that, to reach the good fit between the calculated and experimental EPR parameters,

$$\Delta z \approx 0.2612 \text{ \AA}, \quad \Delta x \approx 0.175 \text{ \AA}. \quad (7)$$

The comparisons between the calculated and observed EPR parameters are shown in Table 1.

3. Discussion

The above studies suggest that the local structures (characterized by the displacements Δz and Δx) of impurity centers for V³⁺ and Cr⁴⁺ ions in Al₂O₃ crystals are different from the corresponding structure in the host Al₂O₃ crystal. The directions of the impurity displacement Δz and the O²⁻ displacement Δx are consistent with the expectation based on the electrostatic interaction model. In addition, considering that the electrostatic repulsive force between a Cr⁴⁺-Al³⁺ pair in Al₂O₃ is larger than that between a V³⁺-Al³⁺ pair because of more charge of the Cr⁴⁺ ion, the impurity displacement Δz (and hence the O²⁻ displacement Δx) in Al₂O₃:Cr⁴⁺ may be bigger than that in an Al₂O₃:V³⁺ crystal. This point is supported by the above calculations. So, the local structures of V³⁺ and Cr⁴⁺ centers in Al₂O₃ crystals obtained above can be regarded as suitable. Based on these local structures, the EPR parameters D , g_{\parallel} and g_{\perp} for both centers in Al₂O₃ are reasonably explained.

Acknowledgement

This project was supported by the Scientific Research Foundation of the Chongqing Institute of Technology of China (Grant No. 2005Z077) and the CAAC Scientific Research Base of Civil Aviation Flight Technology and Safety.

- [1] C. A. Morrison, *Crystal Field for Transition-Metal Ions in Laser Host Materials*, Springer, Berlin 1992.
- [2] N. P. Barnes, J. A. Williams, J. C. Barnes, and G. E. Lockard, *IEEE J. Quantum Electron.* **24**, 1021 (1998).
- [3] P. F. Moulton, *Laser Focus* **23**, 56 (1987).
- [4] T. H. Maiman, *Nature* **187**, 493 (1960).
- [5] M. Abou-Ghantous, C. A. Bates, and L. C. Goodfellow, *J. Phys. Chem. Solids* **37**, 1059 (1976).
- [6] J. Pontnau and R. Adde, *J. Phys. Chem. Solids* **36**, 1023 (1975).
- [7] R. R. Joyce and P. L. Richards, *Phys. Rev.* **179**, 375 (1969).
- [8] G. M. Zverev and A. M. Prokhorov, *Sov. Phys. JETP* **13**, 714 (1961).
- [9] D. S. McClure, *J. Chem. Phys.* **38**, 2289 (1963).
- [10] S. Sugano, Y. Tanabe, and H. Kamimura, *Multiplets of Transition-Metal Ions in Crystals*, Academic Press, New York 1970.
- [11] W. L. Feng, X. X. Wu, and W. C. Zheng, *Phys. Status Solidi B* **243**, 1881 (2006).
- [12] A. Abragam and B. Bleaney, *Electron Paramagnetic Resonance of Transition Metal Ions*, Oxford University Press, London 1970.
- [13] J. S. Griffith, *The Theory of Transition-Metal Ions*, Cambridge University Press, London 1964.
- [14] J. A. Lever, *Inorganic Electronic Spectroscopy*, Elsevier, Amsterdam 1984.

- [15] Z. Y. Yang, C. Rudowicz, and J. Qin, *Physics B* **318**, 188 (2002).
- [16] W. C. Zheng, Q. Zhou, X. X. Wu, and Y. Mei, *Spectrochim. Acta A* **61**, 1243 (2005).
- [17] D. J. Newman and Ng Betty, *Rep. Prop. Phys.* **52**, 699 (1989).
- [18] W. L. Yu, X. M. Zhang, L. X. Yang, and B. Q. Zen, *Phys. Rev. B* **50**, 6756 (1994).
- [19] X. X. Wu, W. C. Zheng, and S. Tang, *Z. Naturforsch.* **59a**, 47 (2004).
- [20] M. H. L. Pryce and W. A. Runciman, *Discuss. Faraday Soc.* **26**, 34 (1958).
- [21] W. C. Scott and M. D. Sturge, *Phys. Rev.* **146**, 262 (1966).
- [22] C. Rudowicz and Y. Y. Zhou, *J. Magn. Magn. Mater.* **111**, 153 (1992).
- [23] M. G. Zhao, J. A. Xu, G. R. Bai, and H. S. Xie, *Phys. Rev. B* **27**, 1516 (1983).
- [24] K. H. Karlsson and T. Perander, *Chem. Scr.* **3**, 201 (1973).